Anaerobic granular sludge-derived activated carbon: preparation, characterization and superior dye adsorption capacity

Ge Zhang[a], Tao Yan[a], Dong Wei[a], Liangguo Yan[a], Xiaodong Wang[a], Qin Wei[b], Bin Du[a],*

[a]*School of Resources and Environment, University of Jinan, Jinan 250022, P.R. China, emails: zhangge8906@163.com (G. Zhang), yantujn@163.com (T. Yan), weidong506@163.com (D. Wei), yanyu_33@163.com (L. Yan), wangxdujn@163.com (X. Wang), Tel./Fax: +86 531 8276 7370; email: dubin61@gmail.com (B. Du)*
[b]*Key Laboratory of Chemical Sensing & Analysis in Universities of Shandong, School of Chemistry and Chemical Engineering, University of Jinan, Jinan 250022, P.R. China, email: sdjndxwq@163.com*

ABSTRACT

Anaerobic granular sludge-derived activated carbon (AGSC) was prepared as a novel adsorbent for the removal of malachite green (MG) from aqueous solution. The composition and structure of AGSC were characterized by Fourier transform infrared spectroscopy, N_2 adsorption–desorption isotherms, Scanning electron microscope, Zeta potential, and X-ray photoelectron spectroscopy. Adsorption capacity of MG onto AGSC was investigated in a batch system by considering the effects of various parameters including pH value, adsorbent dose, contact time, and temperature. AGSC exhibited a high surface area (741.1 m^2/g) and adsorption capacity (304.9 mg/g). The pseudo-second-order kinetic model and the Langmuir model could well explain the adsorption processes of AGSC. Thermodynamic parameters of the adsorption processes, such as ΔG (−2.23 kJ/mol), ΔH (5.50 kJ/mol K) and ΔS (25.8 J/mol K), were also calculated. The negative ΔG and the positive ΔH indicated that the adsorption was spontaneous and endothermic. The result of this study could provide strong evidence for the potential of adsorbent in removing pollutant from wastewater.

Keywords: Activated carbon; Malachite green; Adsorption; Kinetics; Thermodynamic

1. Introduction

Various technologies have been applied to remove pollution such as dye, heavy metals, and organic compounds from wastewater [1,2]. Adsorption is one of an attractive method due to low cost, simplicity of design and operation for water treatment [3]. Among the adsorption researches, activated carbon (AC), the most frequently-used adsorbing material, was widely applied in wastewater treatment because of their exceedingly porous and large surface area, fast adsorption kinetics, and high adsorption capacities [4,5]. However, the high cost of AC production is a huge challenge for commercial manufacturers. In recent years, some studies have focus on the inexpensive precursory materials with high carbon content including *Eucalyptus camaldulensis* wood [6], olive fruit stones [7], African biomass residues [8], lignocellulosic biomass [9], sludge [10], and agroindustry waste [11].

*Corresponding author.

Sludge which is a byproduct produced from numerous industrial activities has been recognized as an ecological burden for the society. However, viewing the sludge, as a carbon-rich material, has stimulated new gateways for the production of porous ACs for water treatment applications [12]. This pattern would not only solve the disposal problem of the sludge but also turn solid waste into an efficient adsorbent.

Anaerobic granular sludge is a dense microbial community that typically includes millions of organisms per gram of biomass. Anaerobic treatment is the history wastewater treatment and has been rapidly developed since the late 1960s. The dense microbial aggregates and densities are much higher than the conventional activated sludge. McHugh et al. suggested that the application of anaerobic granular sludge was regarded as one of the promising biotechnologies in wastewater treatment [13]. In addition, anaerobic treatment processes are more cost-effective than aerobic treatment processes for high concentration of organic wastewater in WWTPs [14]. In future, this technology would be more widely applied and it is expected that anaerobic granular sludge would be used as a potential carbon-rich precursor for the preparation of AGSC. More detail, extracellular polymeric substances (EPS) which are composed of complex high-molecular weight mixture of polymers are essential for keeping microbial aggregates together in anaerobic granular sludge. Polysaccharides and proteins are the major components of EPS that contains a large number of functional groups, including hydroxyl, carboxyl and amino groups, which bind with contaminant molecules easily. Therefore, the preparation of AGSC by anaerobic granular sludge has a desirable prospect.

In addition to the selection of precursory materials, the activation process of preparation method has significant effects on the pore structure and adsorption capacity of AC. AC could be produced by three different processes including physical activation, chemical activation, and physical–chemical activation [15]. Physical activation involves gas-activating agents such as steam and CO_2. Chemical activation is a dehydrating agent, such as KOH, H_3PO_4 and $ZnCl_2$, and then activated at high temperatures under an inert atmosphere. Compared with physical activation method, the chemical activation technique has many merits including lower activation temperature, shorter heat treatment, and higher carbon yield [16]. In addition, different chemical activating reagents have significant effects on the physicochemical characteristics of carbon production. $ZnCl_2$ is a widely used activation agent that results in a high surface area and more micropore structure [17]. $ZnCl_2$ activation causes electrolytic action termed as "swelling" in the molecular structure of cellulose, which dissolve cellulose resulting in increased inter- and intra-voids. It also promotes the development of porous structure of the AC because of the formation of small elementary crystallites. A similar $ZnCl_2$ activation method has been reported by Subha and Namasivayam, in which coir pith carbon was produced and used as a low adsorbent for the removal of 2,4-dichlorophenol [18].

In this study, a novel activated carbon (AGSC) was prepared from anaerobic granular sludge by chemical activation with zinc chloride. Malachite green (MG) was selected as a target pollutant to explore the adsorption performance of AGSC. MG is extensively utilized as a parasiticide, fungicide, and bactericide in aquaculture industries worldwide [19,20]. The effects of different parameters including adsorbent dose, pH value, contact time and temperature were studied to optimize the adsorption process. In order to further explore the interaction between AGSC and MG, the kinetics, isotherms, thermodynamic, and mechanism were also studied.

2. Materials and methods

2.1. Materials

2.1.1. Reagents

The chemicals, which were obtained from Sinopharm Chemical Reagent Beijing Co. Ltd, China, were of analytical reagent grade without further purification. Ultrapure water (EASY-pure LF, Barnstead International, Dubuque, IA, USA) was used throughout the experiment.

2.1.2. Apparatus

The N_2 adsorption–desorption isotherms and pore size distribution of AGSC was characterized with an automated gas sorption apparatus (Micromeritics ASAP 2020 system, USA) under nitrogen adsorption–desorption isotherms at 77 K. The surface morphology of AGSC was observed using a scanning electron microscope (SEM) (JEOL JSM-6700F microscope, Japan). The surface functional groups of AGSC were analyzed by the Fourier transforms infrared (FTIR) spectroscopy (VERTEX70 spectrometer, Bruker Co. Germany). Zeta potential was measured by a Malvern zetameter (Zetasizer 2000). The surface binding state and elemental speciation of AGSC were analyzed by X-ray photoelectron spectroscopy (XPS) (ESCALAB 250).

2.2. Preparation of AGSC

In this study, anaerobic granular sludge was obtained from a factory of soy protein in Shandong province. The raw sewage sludge was dried at 100°C for 24 h to achieve constant weight. Then, sample was crushed and activated by zinc chloride. Subsequently, the anaerobic granular sludge was carbonized at 650°C in a tube furnace for 2 h under nitrogen atmosphere and then cooled to room temperature. The AGSC was washed with hydrochloric acid and distilled water, then dried at 100°C for 12 h. The dried sample was grinded, and stored in a desiccator until required.

2.3. Dye adsorption

The dye solution (1,000 mg/L) of MG was prepared by dissolving 1 g MG of accurately weighed in 1,000 mL distilled water. All working solutions with desired concentrations were prepared by dilution with distilled water. The adsorption experiments were carried out in order to evaluate the effects of solution pH, adsorbent dose, and time. The adsorption studies were performed by mixing 12 mg of AGSC and 60 mL of MG solution under mechanical shock in a water bath shaker. The residual concentration of dye was analyzed by spectrophotometer at 618 nm. The pH of the dye solution was adjusted using HCl or NaOH (1 mol/L). The amount of adsorbents was also investigated in the range of 2–16 mg/60 mL. For adsorption isotherm, the mixture concentrations of dye solutions (25–260 mg/L) and adsorbent (12 mg) were stirred at 298, 308, 318, and 328 K until the adsorption reached equilibrium.

The removal efficiency and the amount of MG adsorbed q_t (mg/g) were given according to the following Eqs. (1) and (2):

$$\text{Removal efficiency } (\%) = \frac{(C_0 - C_t)}{C_0} \times 100\% \tag{1}$$

$$q_t = \frac{(C_0 - C_t)V}{W} \tag{2}$$

where C_t (mg/L) is the concentration of adsorbate at time t (min), V (L) is the volume of adsorbate solution, W (g) is the mass of adsorbents, q_t (mg/g) is the adsorbed amount at time t (min).

3. Results and discussion

3.1. Characterization of AGSC

Fig. 1 shows the pore size distribution and nitrogen adsorption/desorption isotherm of AGSC. The surface area, total pore volume, and average pore diameter of the AGSC were 741.1 m^2/g, 0.30 cm^3/g and 3.60 nm, respectively. The nitrogen adsorption–desorption isotherm belongs to the type IV according to the International Union of Pure and Applied Chemistry (IUPAC) classification, indicating the presence of mesoporous [21]. The surface morphology of the AGSC was characterized by SEM. Fig. 2 shows the surface of AGSC was loose and multihole at different magnifications. Therefore, it can achieve more surface area available for adsorption [22]. These holes were resulted from the evaporation of impregnates ZnCl$_2$ derived compounds, leaving the space previously occupied by the reagent [23].

3.2. Influence of adsorbent dose

The effect of adsorbent dose on the removal of MG by AGSC was showed in Fig. 3(a). It could be seen that the removal percentage varied from 75 to 95 when adsorbent dose ranging from 2 to 16 mg. This could be attributed to the increase availability of more adsorption sites and sorbent surface area [24]. However, the dyes removal could not be significantly improved when the adsorbent dose was more than 12 mg, due to the decrease in total adsorption surface area available to MG resulting from overlapping or aggregating of adsorption sites [25]. Considering the removal efficiency and practicality, an adsorption dose of 12 mg was selected as the optimum adsorbent for the following studies.

3.3. Effect of pH

The effect of initial pH values on the removal of MG by AGSC was carried out by detecting the absorbance of the dye solution with the pH values in the range from 3.0 to 10.5. The dye solutions were obtained as follows: Firstly, the pH value of dye solution with initial dye concentration of 10 mg/L was adjusted by HCl or NaOH. Secondly, 12 mg of adsorbent (AGSC) was added in the dye solution and the adsorption reaction was allowed to continue for 2.5 h at 25°C under stirring. The adsorption of MG onto AGSC increased from 49.2 to 57.8 mg/L with an increase in the pH value and showed a good adsorption performance over a wide pH range from 5.0 to 8.5 (Fig. 3(b)). Nevertheless, when the pH value was greater than 8.5, the color of dye solution fades immediately without stirring, which could attribute to the structural changes of MG molecules at higher pH values [26].

At low pH value, the high concentration of H$^+$ ions accelerated the protonation of the functional groups
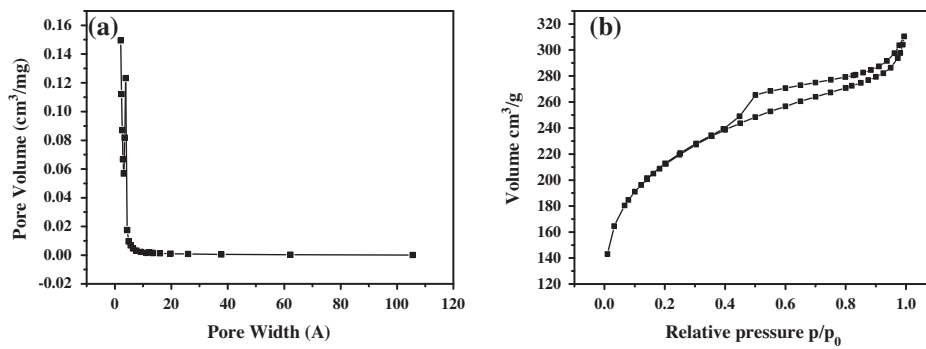
Fig. 1. (a) Pore size distribution and (b) nitrogen adsorption–desorption isotherm of AGSC.
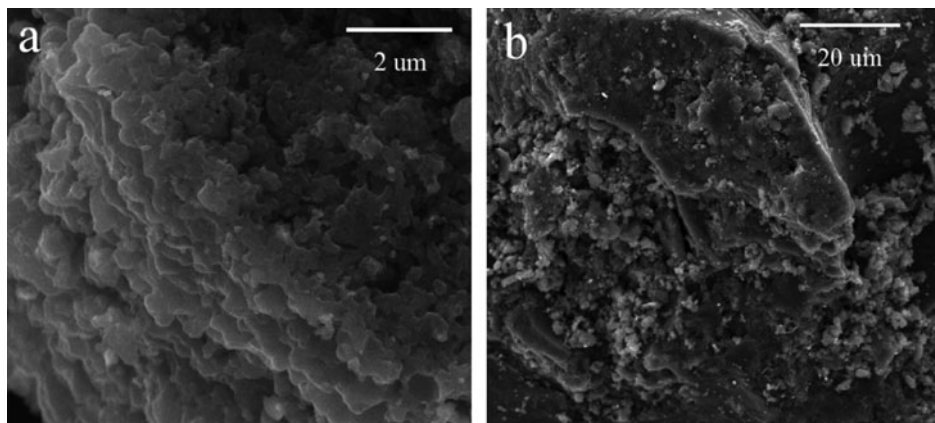
Fig. 2. (a and b) SEM images of AGSC (different scale).

easily, thereby the adsorbent became more positively charged. There was a repulsion force between the cationic MG molecules and the adsorbent surface. Furthermore, excessive H^+ ions would compete with positively charged MG molecules for the adsorption sites, so the adsorption capacity of MG decreased greatly at low solution pH values. However, with an increase in the of pH value, dye cations were easily anchored on the adsorbent surface due to weakness of the competition. Therefore, the removal efficiency of MG increased at high pH value [27].

3.4. Adsorption kinetics

It was essential to evaluate the effect of contact time required to reach equilibrium for designing batch adsorption experiments. Fig. 3(c) shows the effect of contact time on the MG adsorption by the AGSC. The MG adsorption rates increased dramatically in the first 10 min and then slowly increased. The adsorption reached equilibrium at 150 min.

Several kinetic models, such as pseudo-first-order model, pseudo-second-order kinetic model, and the intra-particle diffusion, were used to evaluate adsorption kinetics. The kinetic models for MG adsorption on AGSC are displayed in Fig. 4.

The pseudo-first-order Lagergren equation [28] was expressed as follows Eq. (3):

$$\log (q_e - q_t) = \log q_e - \frac{k_1}{2.303}t \tag{3}$$

where q_t and q_e (mg/g) are the amount adsorbed at time t and at equilibrium and k_1 (min^{-1}) is the pseudo-first-order rate constant for the adsorption process.

The pseudo-second-order model Eq. (4) can be expressed in the following form [29]:

$$\frac{t}{q_t} = \frac{1}{k_2 q_e^2} + \frac{1}{q_e}t \tag{4}$$

where k_2 (g/mg min) is the pseudo-second-order rate constant.
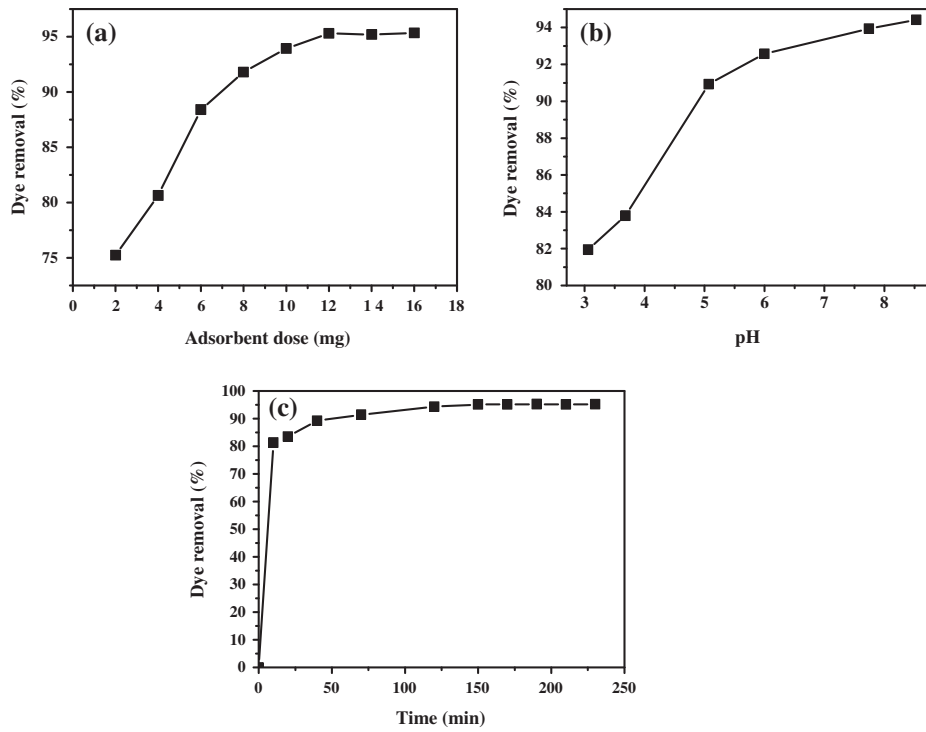
Fig. 3. Effect of adsorbent dose (a), solution pH (b), and contact time (c) on the adsorption of MG by AGSC.
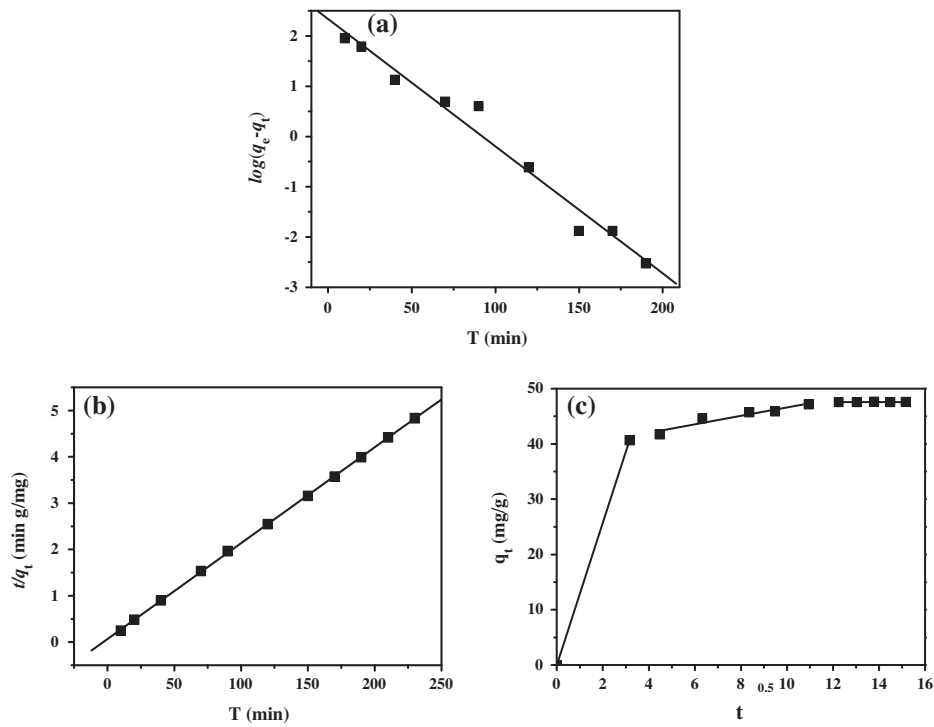
Fig. 4. (a) Pseudo-first-order kinetics plots, (b) Pseudo-second-order kinetics plots, and (c) Intra-particle diffusion plots for MG onto AGSC.

Parameters of pseudo-first-order and pseudo-second-order models for the adsorption of MG onto AGSC are given in Table 1. The R^2 values for pseudo-second-order kinetic model were higher than that of the pseudo-first-order model. For pseudo-second-order equation, the calculated q_e value was much closer to the experimental q_e value. However, the calculated q_e value of pseudo-first-order equation differed a lot. Therefore, the adsorption of MG onto AGSC can be well described by the pseudo-second-order model and which supported the assumption for the model due to chemisorption [28].

The intra-particle diffusion model was applied to determine if the rate-limiting step was intra-particle diffusion. The solute transfer process was usually characterized by external mass transfer or intra-particle diffusion, especially for a solid–liquid adsorption process [30]. The rate parameter for intra-particle diffusion Eq. (5) was expressed as follows:

$$q_t = k_{int}t^{1/2} + C \qquad (5)$$

where k_{int} (mg/g min$^{1/2}$) is the intra-particle diffusion rate constant and C (mg/L) is the intercept.

The intra-particle diffusion plot is shown in Fig. 4(c), it was evident that the adsorption process follows three steps. The first region was very sharp and indicated rapid attachment of MG molecules to the external surface of the AGSC. The second linear region was the gradual adsorption stage signifying the rate-limiting step being the intra-particle diffusion of the adsorbate molecules. The third region showed the final equilibrium stage where MG diffusion was very slow due its low concentration [31]. It could be seen that the linear lines of the second and third stages did not pass through the origin. Therefore, intra-particle diffusion was not the only rate limiting-step and the main chemisorption may be involved in the process [32].

3.5. Influence of dye concentration at different temperatures

The adsorption isotherms, 12 mg of AGSC was taken with 60 mL of MG at different concentrations (25–260 mg/L) in a water bath shaker for equilibrium at 298, 308, 318, and 328 K. The results are showed in Fig. 5, respectively. The value of q_e increased with an increase in the concentration. This was because the increased concentration gradient driving force. Furthermore, the value of q_e increased with the increasing temperature, indicating the process was endothermic.

3.6. Adsorption isotherms

In this study, the equilibrium data for adsorption of MG on AGSC were analyzed using the Freundlich and Langmuir isotherms.

The linear form of Freundlich isotherm equation (Eq. (6)) was [33]:

$$\ln q_e = \ln K_F + \frac{1}{n}\ln C_e \qquad (6)$$

The linear form of Langmuir isotherm equation (Eq. (7)) was [34]:

$$\frac{C_e}{q_e} = \frac{C_e}{q_m} + \frac{1}{K_L q_m} \qquad (7)$$

where q_e (mg/g) is the amount of dye adsorbed at equilibrium, C_e (mg/L) is the equilibrium dye concentration in solution, K_F ((mg/g)(l/mg)$^{1/n}$) is the Freundlich constant, and $1/n$ is the heterogeneity factor, respectively. If $1 < 1/n$, this means poor adsorption; $0.5 < 1/n < 1$ means moderately difficult adsorption; and $0.1 < 1/n < 0.5$ good adsorption. The higher the n value the stronger the adsorption intensity [35]. Where q_m (mg/g) is monolayer adsorption capacity, K_L (L/mg) is Langmuir isotherm constant.

The essential feature of a Langmuir isotherm can be expressed in accordance with a dimensionless constant separation factor or equilibrium parameter Eq. (8), R_L, which was defined by [36]:

$$R_L = \frac{1}{1 + K_L C_0} \qquad (8)$$

Table 1
Parameters of pseudo-first-order and pseudo-second-order models for the adsorption of MG onto AGSC.

C_0 (mg/L)	$q_{e,exp}$ (mg/g)	Pseudo-first-order		
10	47.7	k_1 (min^{-1}) 0.0253	$q_{e,cal}$ (mg/g) 10.4	R^2 0.9754
10	47.7	k_2 (g/mg min) 0.0066	$q_{e,cal}$ (mg/g) 48.3	R^2 0.9990
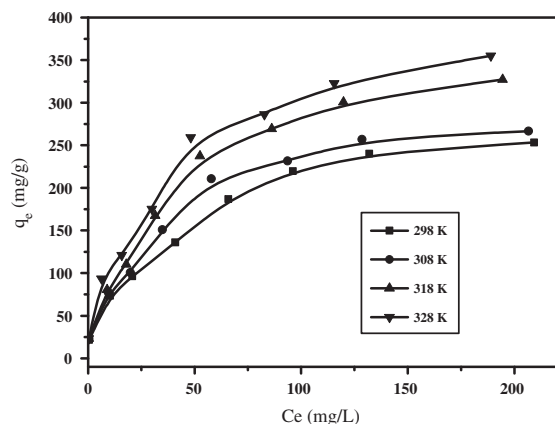
Fig. 5. MG adsorption isotherm on the AGSC at different temperatures.

where C_0 (mg/L) is the initial dye concentration and K_L (L/mg) is Langmuir isotherm constant. The R_L values indicate the type of the isotherm be unfavorable ($R_L > 1$), linear ($R_L = 1$), favorable ($0 < R_L < 1$), irreversible ($R_L = 0$).

The values of constants obtained from the two models are shown in Table 2. It could be seen the Langmuir model (R^2, at a range between 0.9902 and 0.9959) fits better than the Freundlich model (R^2, at a range between 0.9619 and 0.9692), indicating the monolayer coverage of MG onto AGSC. The value of R_L in the range of 0–1 indicating the adsorption process was very favorable. The values of $1/n$ were less than 1 for all temperatures indicating the adsorption was beneficial [25]. The values of K_F and q_m increased with increasing temperature indicating that the adsorption process was endothermic.

Table 3 shows the comparison of the maximum adsorption capacities of MG onto various adsorbents.

Although the published values were obtained under different experimental conditions, they may be useful as a criterion for comparing the adsorption capacities. It could be seen that the adsorption capacity of AGSC obtained in this work was larger than other biological adsorbents. The yield of the AGSC is not high (about 35%), but the high surface area and surface functionality could significantly increase the adsorption capacity of AGSC. In addition, it is a potential application of adsorption material due to the low cost and ease to synthesis.

3.7. Thermodynamic parameters

Thermodynamic parameters Eqs. (9–10) such as standard free energy (ΔG), enthalpy (ΔH), and entropy (ΔS) were calculated using the following equations [44]:

$$\Delta G = -RT \ln K_d \tag{9}$$

$$\ln K_d = \Delta S/R - \Delta H/RT \tag{10}$$

where R (8.314 J/mol K) is the gas constant, T is absolute temperature in K, and K_d is the equilibrium constant. The K_d Eq. (11) was calculated by the following equation [45,46]:

$$K_d = q_e/C_e \tag{11}$$

where q_e is amount of MG (mg) adsorbed by one gram of AGSC at equilibrium, C_e (mg/L) is the equilibrium concentration of MG in solution.

The calculated parameters are presented in Table 4, and the negative values of ΔG and positive values of ΔH indicated that sorption of MG onto AGSC was

Table 2
Isotherm parameters for adsorption of MG at different temperatures.

	Temperature (K)			
	298	308	318	328
Freundlich				
K_F $((mg/g)(l/mg)^{1/n})$	26.52	28.30	29.62	41.79
$1/n$	0.4465	0.4571	0.4833	0.4274
R^2	0.9666	0.9692	0.9619	0.9660
Langmuir				
q_m (mg/g)	304.9	347.2	396.8	413.2
K_L (l/mg)	0.0250	0.0237	0.0249	0.0306
R_L	0.1333–0.6154	0.1394–0.5129	0.1337–0.6163	0.1120–0.4499
R^2	0.9937	0.9930	0.9959	0.9902

Table 3
The comparison of the maximum adsorption capacities of MG onto various adsorbents

Adsorbents	Adsorption capacities (mg/g)	Refs.
Graphene oxide/cellulose bead	17.8	[37]
$Cd(OH)_2$-NW-AC	19.0	[38]
Iron humate	19.2	[39]
Coconut coir	27.4	[36]
Alg-Fe_3O_4	47.8	[40]
Borassus aethiopum	48.5	[41]
Sewage sludge	49.3	[42]
Effective Micro-organisms	136.6	[43]
Anaerobic granular sludge	304.9	This study

Table 4
Thermodynamic parameters for the adsorption of MG onto AGSC

Temperature (K)	ΔG (kJ/mol)	ΔH (kJ/mol K)	ΔS (J/mol K)
298	−2.23	5.50	25.8
308	−2.42	5.50	25.8
318	−2.55	5.50	25.8
328	−3.06	5.50	25.8

spontaneous and endothermic [47]. With the temperature increasing from 298 to 328 K, the values of ΔG decreased from −2.229 to −3.056 kJ/mol, which indicated that the endothermic adsorption of MG onto AGSC was enhanced by an increase in temperature. The value of ΔH was high enough to ensure strong interaction between the adsorbate and adsorbent. The entropy change (ΔS) was 25.76 J/mol K, which showed an increasing disorder at the interface between MG and AGSC. Similar phenomenon was reported by Rakhshaee et al., in which magnetic nanoadsorbent was used to removal methylene blue [48]. The adsorption capacity increased at higher temperature may be caused by the enlargement of pore size and activation of the adsorbent surface [49].

3.8. Adsorption mechanism

Zeta potential of AGSC before and after dye sorption was measured at various pH values and was showed in Fig. 6. The isoelectric points (pHzpc) of AGSC were 4.8, indicating that the surface of AGSC was positive under pH 4.8. The great negative zeta potential suggested that positively charged pollutants (MG) may be more easily adsorbed onto AGSC. After MG adsorption, the zeta potentials of AGSC were significantly increased at the same pH values and the isoelectric points shifted to higher pH values of 7.2. These results suggest that electrostatic interaction
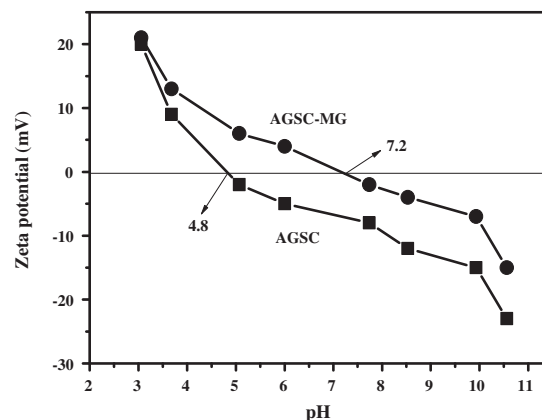
Fig. 6. Zeta potential of AGSC.

attraction may play an important role in the adsorption mechanism.

The characteristic functional groups of adsorbent were investigated using FTIR spectra in the range of 4,000–500 cm^{-1}. In Fig. 7(a), the adsorption band at 3,435 cm^{-1} was the stretching frequency of the hydroxyl group (−OH) in AGSC functional group [50]. Two strong peaks at 2,963 and 2,853 cm^{-1} correspond to C–H bands of methyl and methylene groups [51]. The peaks at 1,610, 1,384, and 1,104 cm^{-1} correspond to asymmetric stretching vibration of −COO, C–N and C–O, respectively. After adsorption of MG, some new
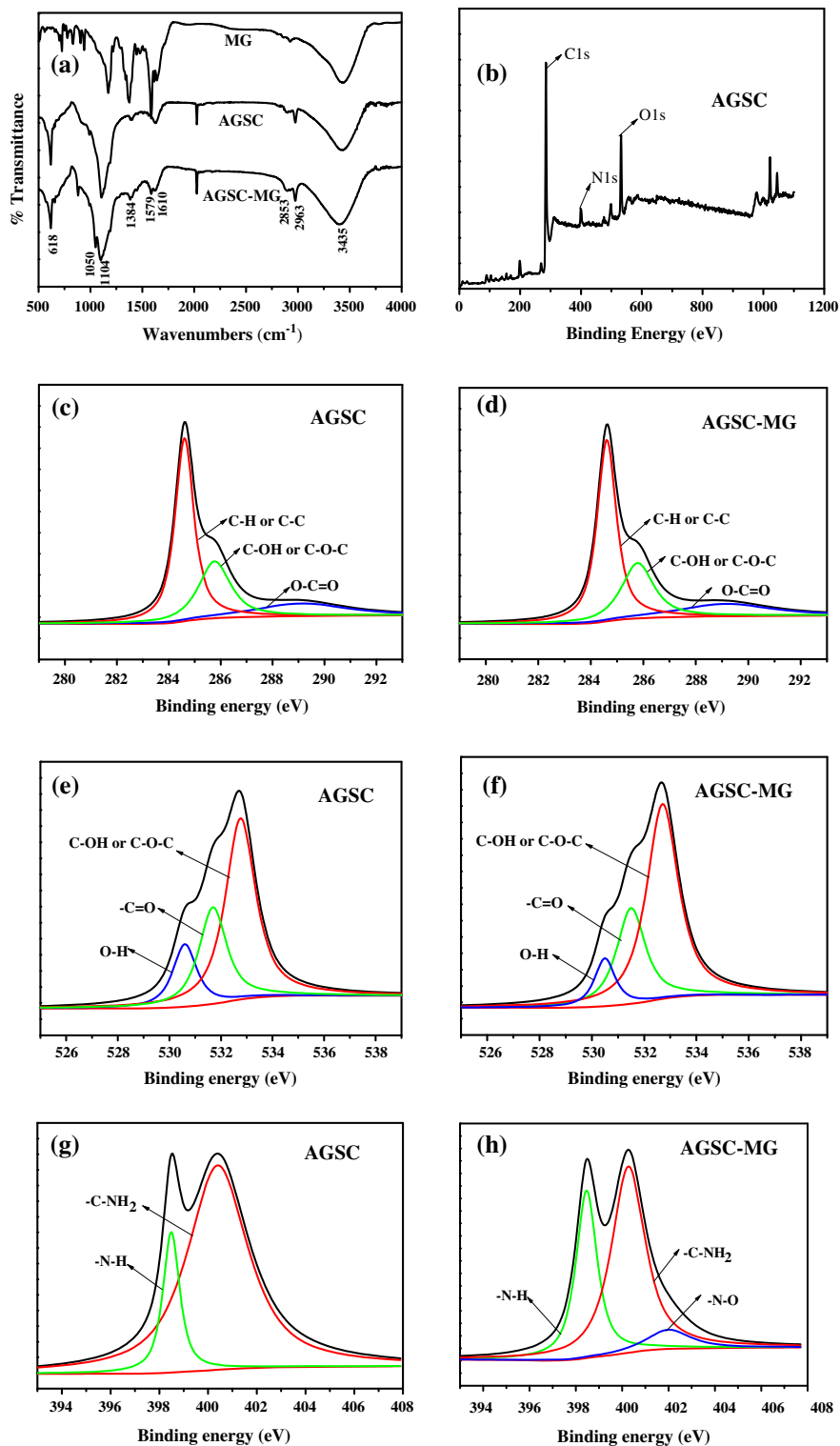
Fig. 7. (a) The infrared spectrum and (b) XPS spectra of AC, (c–h) C 1s, O 1s and N 1s XPS spectra of AGSC and AGSC-MG.

Table 5
Peak numbers and RA of the surface functional groups determined by C 1s, O 1s and N 1s spectra from XPS for AGSC and AGSC-MG

Sample		AGSC			AGSC-MG		
		Peak 1	Peak 2	Peak 3	Peak 1	Peak 2	Peak 3
C 1s	BE (eV)	284.6	285.7	289.0	284.6	285.7	289.0
	RA (%)	53.3%	28%	18.7%	54.7%	27.6%	17.7%
O 1s	BE (eV)	530.4	531.6	532.6	530.4	531.6	532.6
	RA (%)	15.5%	27.8%	56.7%	9.9%	27.7%	62.4%
N 1s	BE (eV)	398.4	400.4	402.0	398.4	400.4	402.0
	RA (%)	16%	79%	5%	33.3%	58.7%	8%

absorption bands occurred on dye-loaded AGSC. The band at 1,579 cm^{-1} corresponds to aromatic ring [52] which exists in the structural formula of MG, indicating MG was adsorbed onto AGSC. The band at 1,050 cm^{-1} corresponds to N–O (no exist in MG and AGSC) [53], indicating surface functionality played an important role in MG adsorption.

The XPS analysis was also performed for AGSC and MG adsorbed AGSC. Analyses of C1s, O1s, and N1s peaks on AGSC and AGSC-MG are presented in Fig. 7(c–h). It revealed that the major C1s peak could be fitted to three curves from the following groups: C–C or C–H at 284.6 eV; C–OH or C–O–C at 285.7 eV; O–C=O at 289 eV. The O1s spectra were fitted to three components corresponding to: O–H at 530.4 eV; C=O at 531.6 eV; C–O or C–O–C at 532.6 eV [54]. The N1s spectra were fitted to three components corresponding to: N–H at 398.4 eV; CNH$_2$ at 400.4 eV; N–O at 402 eV [55]. According to the area-simulating curve, the percentage of each component was calculated and listed in Table 5. The relative area (RA) of peaks 1(O 1s) of AGSC-MG surface decreased slightly compared with that of original AGSC, indicating that the O atom of HO–C=O was electron donors during the N$^+$ atom of MG. The mechanism also could be confirmed by the increase of the RA of peaks 3 (N1s) after MG sorption, which corresponding to the result the adsorption bands at 1,050 cm^{-1} (N–O) in FTIR spectra.

4. Conclusion

In this study, AGSC from anaerobic granular sludge was successfully prepared by zinc chloride activation and used for MG adsorption. AGSC exhibited a high surface area and adsorption capacity. The adsorption capacities are significantly influenced by the contact time, pH value, adsorbent dose, and temperature. The adsorption process could be well fitted by the pseudo-second-order kinetic model. The adsorption data fitted Langmuir isotherm better than Freundlich isotherm. Thermodynamic study showed that the adsorption process was spontaneous and endothermic. The results of this study showed that AGSC could be applied as a novel adsorbent in wastewater treatment for the removal of MG.

References

[1] S. Timur, I.C. Kantarli, S. Onenc, J. Yanik, Characterization and application of activated carbon produced from oak cups pulp, J. Anal. Appl. Pyrolysis 89 (2010) 129–136.
[2] R. Hoseinzadeh Hesas, W.M.A. Wan Daud, J.N. Sahu, A. Arami-Niya, The effects of a microwave heating method on the production of activated carbon from agricultural waste: A review, J. Anal. Appl. Pyrolysis 100 (2013) 1–11.
[3] Y. Li, Q. Du, T. Liu, X. Peng, J. Wang, J. Sun, Y. Wang, S. Wu, Z. Wang, Y. Xia, L. Xia, Comparative study of methylene blue dye adsorption onto activated carbon, graphene oxide, and carbon nanotubes, Chem. Eng. Res. Des. 91 (2013) 361–368.
[4] E. Bulut, M. Özacar, İ.A. Şengil, Adsorption of malachite green onto bentonite: Equilibrium and kinetic studies and process design, Microporous Mesoporous Mater. 115 (2008) 234–246.
[5] C. Djilani, R. Zaghdoudi, F. Djazi, B. Bouchekima, A. Lallam, A. Modarressi, M. Rogalski, Adsorption of dyes on activated carbon prepared from apricot stones and commercial activated carbon, J. Taiwan Inst. Chem. Eng. 53 (2015) 1–10.

[6] A. Heidari, H. Younesi, A. Rashidi, A. Ghoreyshi, Adsorptive removal of CO2 on highly microporous activated carbons prepared from *Eucalyptus camaldulensis* wood: Effect of chemical activation, J. Chin. Inst. Chem. Eng 45 (2014) 579–588.

[7] D. Obregón-Valencia, M.d.R. Sun-Kou, Comparative cadmium adsorption study on activated carbon prepared from aguaje (*Mauritia flexuosa*) and olive fruit stones (*Olea europaea* L.), J. Environ Chem. Eng. 2 (2014) 2280–2288.

[8] M. Gueye, Y. Richardson, F.T. Kafack, J. Blin, High efficiency activated carbons from African biomass residues for the removal of chromium(VI) from wastewater, J. Environ. Chem. Eng. 2 (2014) 273–281.

[9] M.J. Ahmed, S.K. Theydan, Fluoroquinolones antibiotics adsorption onto microporous activated carbon from lignocellulosic biomass by microwave pyrolysis, J. Chin. Inst. Chem. Eng 45 (2014) 219–226.

[10] S.-A. Ong, K. Uchiyama, D. Inadama, Y. Ishida, K. Yamagiwa, Treatment of azo dye Acid Orange 7 containing wastewater using up-flow constructed wetland with and without supplementary aeration, Bioresour. Technol. 101 (2010) 9049–9057.

[11] M.A. Abidin, A.A. Jalil, S. Triwahyono, S.H. Adam, N. Nazirah Kamarudin, Recovery of gold(III) from an aqueous solution onto a *durio zibethinus* husk, Biochem. Eng. J. 54 (2011) 124–131.

[12] P. Hadi, M. Xu, C. Ning, C. Sze Ki Lin, G. McKay, A critical review on preparation, characterization and utilization of sludge-derived activated carbons for wastewater treatment, Chem. Eng. J. 260 (2015) 895–906.

[13] S. McHugh, Anaerobic granular sludge bioreactor technology, Rev. Environ. Sci. Biotechnol. 2 (2003) 225–245.

[14] Q. Yan, D. Yu, Z. Wang, H. Zou, W. Ruan, Phenol inhibition and restoration of the bioactivity of anaerobic granular sludge, Appl. Biochem. Biotechnol. 150 (2008) 259–265.

[15] N. Mohamad Nor, L.C. Lau, K.T. Lee, A.R. Mohamed, Synthesis of activated carbon from lignocellulosic biomass and its applications in air pollution control—A review, J. Environ. Chem. Eng. 1 (2013) 658–666.

[16] B.V. Kaludjerović, V.M. Jovanović, S.I. Stevanović, Ž.D. Bogdanov, Characterization of nanoporous carbon fibrous materials obtained by chemical activation of plane tree seed under ultrasonic irradiation, Ultrason. Sonochem. 21 (2014) 782–789.

[17] M. Makeswari, T. Santhi, Optimization of preparation of activated carbon from *Ricinus communis* leaves by microwave-assisted zinc chloridechemical activation: Competitive adsorption of Ni^{2+} ions from aqueous solution, J. Chem. (2013) 1–12.

[18] R. Subha, C. Namasivayam, Zinc chloride activated carbon coir pith carbon as low adsorbent for removal of 2,4-dichlorophenol, Indian J. Chem. Technol. 16 (2009) 471–479.

[19] B.H. Hameed, M.I. El-Khaiary, Kinetics and equilibrium studies of malachite green adsorption on rice straw-derived char, J. Hazard. Mater. 153 (2008) 701–708.

[20] T. Santhi, S. Manonmani, T. Smitha, Removal of malachite green from aqueous solution by activated carbon prepared from the epicarp of *Ricinus communis* by adsorption, J. Hazard. Mater. 179 (2010) 178–186.

[21] K.Y. Foo, B.H. Hameed, Preparation of activated carbon by microwave heating of langsat (*Lansium domesticum*) empty fruit bunch waste, Bioresour. Technol. 116 (2012) 522–525.

[22] M. Ghaedi, A. Ansari, M. Habibi, A. Asghari, Removal of malachite green from aqueous solution by zinc oxide nanoparticle loaded on activated carbon: Kinetics and isotherm study, J. Ind. Eng. Chem. 20 (2014) 17–28.

[23] K.Y. Foo, B.H. Hameed, Potential of jackfruit peel as precursor for activated carbon prepared by microwave induced NaOH activation, Bioresour. Technol. 112 (2012) 143–150.

[24] S. Nethaji, A. Sivasamy, G. Thennarasu, S. Saravanan, Adsorption of Malachite Green dye onto activated carbon derived from *Borassus aethiopum* flower biomass, J. Hazard. Mater. 181 (2010) 271–280.

[25] J. Zhang, Y. Li, C. Zhang, Y. Jing, Adsorption of malachite green from aqueous solution onto carbon prepared from Arundo donax root, J. Hazard. Mater. 150 (2008) 774–782.

[26] I.D. Mall, V.C. Srivastava, N.K. Agarwal, I.M. Mishra, Adsorptive removal of malachite green dye from aqueous solution by bagasse fly ash and activated carbon-kinetic study and equilibrium isotherm analyses, Colloids Surf., A Physicochem. Eng. Aspects 264 (2005) 17–28.

[27] W.H. Li, Q.Y. Yue, B.Y. Gao, Z.H. Ma, Y.J. Li, H.X. Zhao, Preparation and utilization of sludge-based activated carbon for the adsorption of dyes from aqueous solutions, Chem. Eng. J. 171 (2011) 320–327.

[28] S. Lagergren, Zur theorie der sogenannten adsorption gelöster stoffe (The theory of so-called adsorption solutes), K. Sven. Vetenskapsakad Handl. 24 (1898) 1–39.

[29] Y.S. Ho, G. McKay, Sorption of dye from aqueous solution by peat, Chem. Eng. J. 70 (1998) 115–124.

[30] S.K. Ling, H.Y. Tian, S. Wang, T. Rufford, Z. Zhu, C. Buckley, KOH catalysed preparation of activated carbon aerogels for dye adsorption, J. Colloid Interface Sci. 357 (2011) 157–162.

[31] V.K. Gupta, A. Nayak, S. Agarwal, I. Tyagi, Potential of activated carbon from waste rubber tire for the adsorption of phenolics: Effect of pre-treatment conditions, J. Colloid Interface Sci. 417 (2014) 420–430.

[32] M.A. Ahmad, R. Alrozi, Removal of malachite green dye from aqueous solution using rambutan peel-based activated carbon: Equilibrium, kinetic and thermodynamic studies, Chem. Eng. J. 171 (2011) 510–516.

[33] L. Ding, B. Zou, W. Gao, Q. Liu, Z. Wang, Y. Guo, X. Wang, Y. Liu, Adsorption of Rhodamine-B from aqueous solution using treated rice husk-based activated carbon, Colloids Surf., A Physicochem. Eng. Aspects 446 (2014) 1–7.

[34] Y. Önal, C. Akmil-Başar, Ç. Sarıcı-Özdemir, Investigation kinetics mechanisms of adsorption malachite green onto activated carbon, J. Hazard. Mater. 146 (2007) 194–203.

[35] E. García, R. Medina, M. Lozano, I. Hernández Pérez, M. Valero, A. Franco, Adsorption of azo-dye orange ii from aqueous solutions using a metal-organic framework material: Iron- benzenetricarboxylate, Materials 7 (2014) 8037–8057.

[36] Uma, S. Banerjee, Y.C. Sharma, Equilibrium and kinetic studies for removal of malachite green from aqueous solution by a low cost activated carbon, J. Ind. Eng. Chem. 19 (2013) 1099–1105.

[37] X. Zhang, H. Yu, H. Yang, Y. Wan, H. Hu, Z. Zhai, J. Qin, Graphene oxide caged in cellulose microbeads for removal of malachite green dye from aqueous solution, J. Colloid Interface Sci. 437 (2015) 277–282.

[38] M. Ghaedi, N. Mosallanejad, Study of competitive adsorption of malachite green and sunset yellow dyes on cadmium hydroxide nanowires loaded on activated carbon, J. Ind. Eng. Chem. 20 (2014) 1085–1096.

[39] P. Janoš, Sorption of basic dyes onto iron humate, Environ. Sci. Technol. 37 (2003) 5792–5798.

[40] A. Mohammadi, H. Daemi, M. Barikani, Fast removal of malachite green dye using novel super paramagnetic sodium alginate-coated Fe_3O_4 nanoparticles, Int. J. Biol. Macromol. 69 (2014) 447–455.

[41] S. Nethaji, A. Sivasamy, G. Thennarasu, S. Saravanan, Adsorption of Malachite Green dye onto activated carbon derived from *Borassus aethiopum* flower biomass, J. Hazard. Mater. 181 (2010) 271–280.

[42] L. Leng, X. Yuan, H. Huang, J. Shao, H. Wang, X. Chen, G. Zeng, Bio-char derived from sewage sludge by liquefaction: Characterization and application for dye adsorption, Appl. Surf. Sci. 346 (2015) 223–231.

[43] T. Bhagavathi Pushpa, J. Vijayaraghavan, S.J. Sardhar Basha, V. Sekaran, K. Vijayaraghavan, J. Jegan, Investigation on removal of malachite green using EM based compost as adsorbent, Ecotoxicol. Environ. Saf. 118 (2015) 177–182.

[44] S.K. Milonjic, A consideration of the correct calculation of thermodynamic parameters of adsorption, J. Serb. Chem. Soc. 72 (2007) 1363–1367.

[45] D. Ghosh, K.G. Bhattacharyya, Adsorption of methylene blue on kaolinite, Appl. Clay Sci. 20 (2002) 295–300.

[46] A. Khenifi, Z. Bouberka, F. Sekrane, M. Kameche, Z. Derriche, Adsorption study of an industrial dye by an organic clay, Adsorption 13 (2007) 149–158.

[47] M. Hema, S. Arivoli, Adsorption kinetics and thermodynamics of malachite green dye unto acid activated low cost carbon, J. Appl. Sci. Environ. Manage. 12 (2008) 43–51.

[48] R. Rakhshaee, M. Panahandeh, Stabilization of a magnetic nano-adsorbent by extracted pectin to remove methylene blue from aqueous solution: A comparative studying between two kinds of cross-likened pectin, J. Hazard. Mater. 189 (2011) 158–166.

[49] X. Guo, Q. Wei, B. Du, Y. Zhang, X. Xin, L. Yan, H. Yu, Removal of Metanil Yellow from water environment by amino functionalized graphenes (NH_2-G)-Influence of surface chemistry of NH_2-G, Appl. Surf. Sci. 284 (2013) 862–869.

[50] E. Akar, A. Altinişik, Y. Seki, Using of activated carbon produced from spent tea leaves for the removal of malachite green from aqueous solution, Ecol. Eng. 52 (2013) 19–27.

[51] S. Khattri, M. Singh, Removal of malachite green from dye wastewater using neem sawdust by adsorption, J. Hazard. Mater. 167 (2009) 1089–1094.

[52] L. Zhang, H. Zhang, W. Guo, Y. Tian, Removal of malachite green and crystal violet cationic dyes from aqueous solution using activated sintering process red mud, Appl. Clay Sci. 93–94 (2014) 85–93.

[53] H.C. Alt, H.E. Wagner, Comparative mid- and far-infrared spectroscopy of nitrogen–oxygen complexes in silicon, Physica B 404 (2009) 4549–4551.

[54] H. Liu, X. Wang, G. Zhai, J. Zhang, C. Zhang, N. Bao, C. Cheng, Preparation of activated carbon from lotus stalks with the mixture of phosphoric acid and pentaerythritol impregnation and its application for Ni (II) sorption, Chem. Eng. J. 209 (2012) 155–162.

[55] Y. Zhai, D. Pang, H. Chen, B. Xiang, J. Chen, C. Li, G. Zeng, L. Qiu, Effects of ammonization on the surface physico-chemical properties of sludge-based activated carbon, Appl. Surf. Sci. 280 (2013) 590–597.